

A Study on the Influence of Aluminum Oxide Layer Properties on Contact Formation

Benjamin Gapp, Fabian Geml, Josh Engelhardt and Giso Hahn
University of Konstanz, Department of Physics, 78457 Konstanz, Germany

Authors for Correspondence: Benjamin.Gapp@uni-konstanz.de, Fabian.Geml@uni-konstanz.de, Josh.Engelhardt@uni-konstanz.de, Giso.Hahn@uni-konstanz.de

ABSTRACT: We present an investigation of the contact formation through the widely used passivation layer stack comprised of aluminum oxide (AlO_x) and silicon nitride ($\text{SiN}_y\text{:H}$). The influence of different aluminum oxide layers deposited by either atmospheric pressure chemical vapor deposition (APCVD) or atomic layer deposition (ALD) on contact formation of screen printed silver contact paste on boron emitters is shown. Excellent contact resistivities below $1 \text{ m}\Omega\text{cm}^2$ are achieved for both AlO_x deposition methods. For APCVD based layers, the contact resistivity is independent of the layer thickness within the investigated range of (8...25) nm. Scanning electron microscopy is used to determine and qualitatively examine silver crystallite formation beneath screen printed silver contacts.

Keywords: Contact, CVD Based Deposition, Screen Printing, PERT

1 INTRODUCTION

Highly optimized processes are necessary for cost-efficient Si-based solar cell production. In many strongly developed and industrialized cell concepts, aluminum oxide (AlO_x) plays an important role as a passivation layer i.e., in the $\text{AlO}_x/\text{SiN}_y\text{:H}$ passivation stack due to its layer properties. Specifically, AlO_x deposited in an atmospheric pressure chemical vapour deposition (APCVD) tool is a highly cost-effective alternative compared to the currently implemented solutions, such as atomic layer deposition (ALD) and plasma-enhanced chemical vapour deposition (PECVD). The passivation quality and firing stability, (no significant dependence on peak firing temperature in the given range) of AlO_x layers deposited by APCVD technique has been shown previously [1], surpassing those of ALD layers. Contact formation of Ag paste on these boron emitters [3] passivated by the $\text{AlO}_x/\text{SiN}_y\text{:H}$ layers will be investigated in this distribution. The goal is to reach sufficiently low contact resistivities $< 2 \text{ m}\Omega\text{cm}^2$ for good contact formation. will be shown for boron emitters passivated with APCVD AlO_x & PECVD $\text{SiN}_y\text{:H}$ stacks and PECVD $\text{SiN}_y\text{:H}$ single layers. This shows the feasibility of AlO_x layers deposited in an APCVD tool for use in a variety of solar cell designs. Low contact resistivities are shown for different deposition parameters, layer thicknesses and Ag contact pastes as well as different firing temperature profiles.

AlO_x .

2 EXPERIMENTAL

Phosphorous-doped n-type Cz-Si wafers ($5 \Omega\text{cm}$; $156 \times 156 \text{ mm}^2$) are alkaline textured and cleaned (Piranha etch & HF-dip) with a subsequent BBr_3 gas diffusion. Afterwards, APCVD AlO_x (deposition temperature $500\text{-}650^\circ\text{C}$) or ALD AlO_x (deposition temperature 300°C) was deposited symmetrically on both sides of the samples. After PECVD $\text{SiN}_y\text{:H}$ deposition with thickness adjusted to optimized anti-reflection conditions to finalize the passivation, Ag contact paste structures designed for TLM (transfer length method) measurement were printed and dried in a screen printing process. Wafers were fired in a fast firing belt furnace (peak wafer temperatures: $750\text{-}830^\circ\text{C}$) before measurement of the TLM structures. The structures are

comprised of contact fingers with a length of 1 cm, a finger width of $60 \mu\text{m}$ and varying finger distance (1.0-2.2 mm). Afterwards, HF was used to etch back the passivation layers as well as the glass formed by the Ag contact paste underneath the Ag fingers, allowing for SEM pictures of the surface.

2.1 Variation of AlO_x layer thickness

APCVD reactors provide the (for the intended reactions) necessary energy by thermal heating of the Si substrate. Precursor gases TMA (trimethyl-aluminum) and O_2 react on the Si surface to form an AlO_x layer [2,3]. The properties of the layer, grown in a matter of seconds, are highly dependent on the deposition parameters and differ in structure from ALD based AlO_x layers [4]. To compare the effects of layer thickness of different deposition methods, AlO_x layers with different layer thicknesses have been deposited on p^+ -emitters ($R_{\text{sheet}} = 80 \Omega/\text{sq}$) via APCVD and ALD. The $\text{SiN}_y\text{:H}$ capping layer thicknesses were varied accordingly for each AlO_x layer thickness to achieve comparable ARC properties. APCVD layer thickness was varied by changing the gas flow on the wafer, while ALD layer thickness was changed by increasing the number of reaction cycles. Samples were printed with commercially available Ag contact paste on one side. All samples were fired at a peak substrate temperature of 795°C with a typical firing profile used for firing-through of Ag paste on $\text{SiN}_y\text{:H}$ single layers. All samples were measured via TLM. The contact resistivity ρ_c was determined from TLM data.

2.2 Influence of APCVD Deposition Temperature

As discussed previously in 2.1, many factors can influence APCVD based deposition. A main influence on layer properties is the deposition temperature. Due to the substrate temperature being the main driving factor of the deposition in APCVD reactors, it is expected that changing the substrate temperature during deposition also changes deposition behavior and resulting layer properties. If layer properties, such as density, structure (e.g. extent of deviation from stoichiometric molecular structure), do influence contact formation by changing the etching behaviour of the glass frit, it is expected that a change in deposition temperature influencing the same properties can cause a similar effect. Furthermore, since

the APCVD based deposition, when compared to ALD AlO_x , uses higher temperatures, it stands to reason to study the effect of an increasing thermal budget during layer growth. Layer thickness was kept constant at 15 nm for this experiment. The actual substrate temperature during deposition lies approximately 50° below the given set values. After $\text{SiN}_y\text{:H}$ deposition, TLM structures were printed with a commercially available Ag paste. Additionally, the previously used firing temperature of 795°C is extended to a variation over 4 different firing temperatures in a temperature window between $770\text{--}815^\circ\text{C}$ for each of the mentioned sample groups as to more accurately represent the flexibility required for PERT solar cell firing.

3 RESULTS AND DISCUSSION

3.1 Influence of Atmospheric Treatment

The results of the TLM measurements in dependence of the AlO_x layer thicknesses can be seen in Fig. 1 for APCVD (blue) and ALD (red) based AlO_x . Samples passivated with ALD based AlO_x show a clear dependency of contact resistivity on AlO_x layer thickness, ranging from $< 1 \text{ m}\Omega\text{cm}^2$ at 5 nm up to $> 10 \text{ m}\Omega\text{cm}^2$ at 30 nm (cf. [5]). In a higher thickness range (18–25 nm), samples passivated with APCVD based AlO_x show an increase in contact resistivity from < 1 to $< 3 \text{ m}\Omega\text{cm}^2$. At lower thicknesses, ρ_c of the Ag contact on APCVD based AlO_x does not change significantly. It is therefore likely that there is an influence on contact formation, depending on the one hand on the layer thickness used, and on the other hand on the deposition technique applied. The influence of layer thickness on contact formation can likely be explained by the different etching behaviour of the glass frit with regard to increasing amount of AlO_x substituting $\text{SiN}_y\text{:H}$ in the for ARC application optimized stack. Additionally, this indicates that AlO_x is etched more slowly than $\text{SiN}_y\text{:H}$. A longer etching time within the same applied high temperature step would decrease the available time for Ag crystal formation, which can lead to increased ρ_c . The Al to O ratio might also have an impact on contact formation.

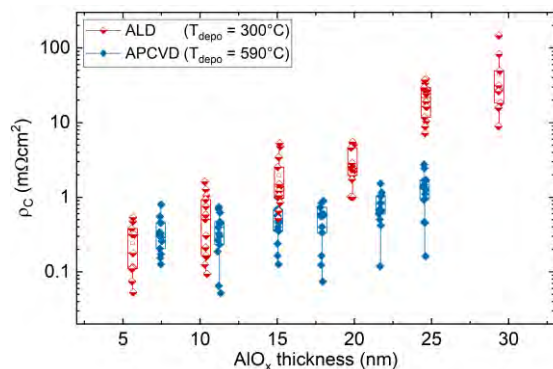


Fig. 1: a) Box-plot diagram of contact resistivity in dependence of AlO_x layer thickness for both APCVD and ALD based AlO_x at a peak firing temperature of 795°C .

To further examine the crystallite growth on the surface, samples with layer thicknesses of 15 and 25 nm APCVD as well as ALD based AlO_x , respectively, have been etched with HF. In this process, the passivation

layers as well as the glass layer below the contact fingers are etched, allowing for an easy removal of the Ag bulk.

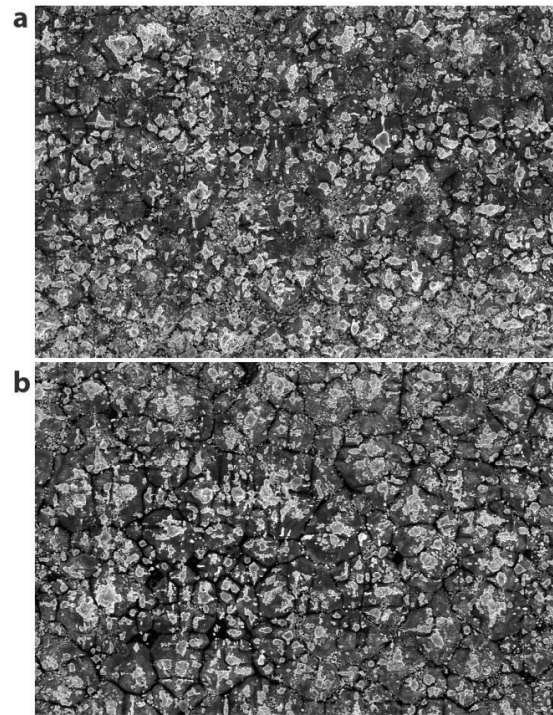


Fig. 2: SEM-pictures of etched surfaces are shown for a) 15 nm and b) 25 nm thick APCVD-based AlO_x layers fired at 795°C . They show bright Ag-crystallites on the dark, textured Si-surface.

SEM pictures of a central finger region underneath the Ag bulk of the underlying surfaces are shown in Figs. 2 and 3 for APCVD and ALD, respectively. In these SEM pictures, Ag crystallites can be seen as bright spots on top of the darker textured Si surface. Typically, etching residuals (e.g. faceted terraces) can also be found on some spots where no crystallites were grown, causing brighter areas in some pictures. Fig. 2 shows a large number of crystallites covering a substantial portion of the depicted area for both layer thicknesses. APCVD based thick layers (25 nm) shown in Fig. 2a show no significant difference in crystallite size and coverage when compared to the lower thickness (15 nm) in Fig. 2b, further supporting the indication made by the contact resistivity values seen in Fig. 1. The crystal growth is typically centered on the top and the edges of almost all texture pyramids. Additional crystallites can be found on the edges between pyramids. In contrast to this, Fig. 3 shows that in the right part of the picture as well as the left, there is a dark area, in which crystallites cover only a smaller portion of the surface. This could explain the small difference between ALD and APCVD even at smaller layer thicknesses. The APCVD based layer in Fig. 2a with the same thickness shows a similar feature, as previously described. In this case, though, areas with limited crystallite growth are less pronounced. A similar comparison of layers with a larger layer thickness (25 nm) in Figs. 2b and 3b can be made. A significant difference in crystallite growth can be found for ALD layers in Fig. 3b compared to Figs. 2a, 2b and 3b. The size and amount of crystallites is drastically decreased. Crystallites of this size are less likely to be in contact with the finger bulk above the glass layer. This large

difference in crystallite size, amount and coverage is therefore likely to be the reason for the difference in ρ_c , depending on the layer thickness. The crystallite size on the Si surface usually depends on the thermal budget left after the overlying layers have been etched. Arguably, Al from an AlO_x layer could influence crystallization and the growth process into the Si surface, by elemental addition to the paste bulk during contact formation, similar to Al in commercially used AgAl contact pastes [6]. However, in this case, deep spiking structures of clearly recognizable “square” shape would be expected if this was the case. No such typical Ag and Al containing crystallite spike structures could be found, making it unlikely for Al from the AlO_x layer to act in its elementary form in this case. As such, the underlying study does not suggest such an influence.

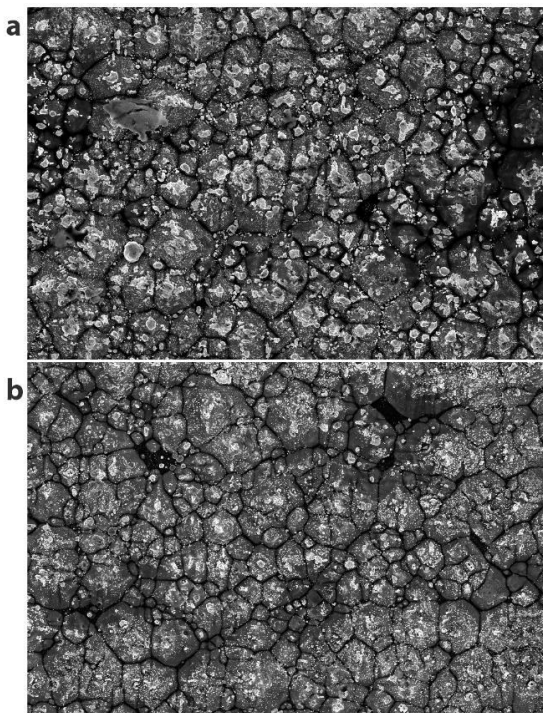


Fig. 3: SEM-pictures of etched surfaces are shown for a) 15 nm and b) 25 nm thick ALD-based AlO_x layers fired at 795°C. They show bright Ag-crystallites on the dark, textured Si-surface.

3.2 Influence of Deposition Temperature on Contact Formation

In the following the influence of APCVD deposition temperature on contact formation will be discussed. Fig. 4 shows the dependence of ρ_c on peak substrate temperature during firing. Different set deposition temperatures during AlO_x ($d_{\text{AlO}_x} = 15 \text{ nm}$) deposition are represented in different colors. Generally, ρ_c remains $< 10 \text{ m}\Omega\text{cm}^2$ for all sample groups. This shows a certain firing stability concerning contact formation over a large temperature window of 45°C for all groups. Both the highest and the lowest deposition temperature show the highest (680°C, black) and lowest (590°C blue) ρ_c throughout the depicted firing temperature range, respectively. In contrast to this, layers deposited at temperatures between 610-650°C (yellow, orange and green) decrease in ρ_c with increasing firing temperature. Contact formation through these layers is similar to the

590°C layer at high firing temperatures, while at low firing temperatures, all layers except the 590°C layer remain above $2 \text{ m}\Omega\text{cm}^2$ in ρ_c . A large difference in ρ_c between highest and lowest deposition temperature at 795°C peak firing temperature is likely due to different properties of the layers. A hotter deposition could accelerate the deposition on the one hand, causing lower density of the layer. At the same time, a heated up AlO_x might be more likely to undergo a restructuring process during and immediately after deposition, which could cause higher layer density. ALD based layers, which are likely to be of higher density due to the much lower deposition rate, have shown higher ρ_c . Therefore, the second explanation is more likely.

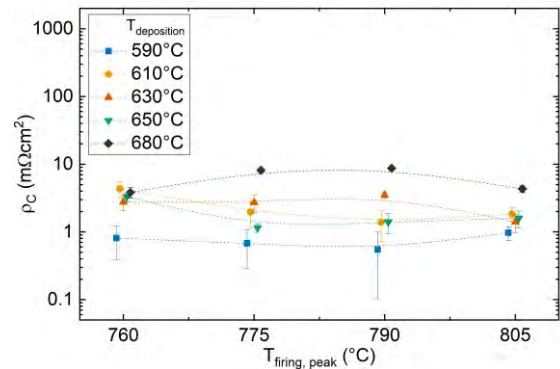


Fig. 4: Contact resistivity in dependence of peak substrate firing temperature for different set temperatures during APCV-deposition of AlO_x layer (different colors representing deposition temperature in APCVD tool, with guides-to-the-eye) with constant $d_{\text{AlO}_x} = 15 \text{ nm}$.

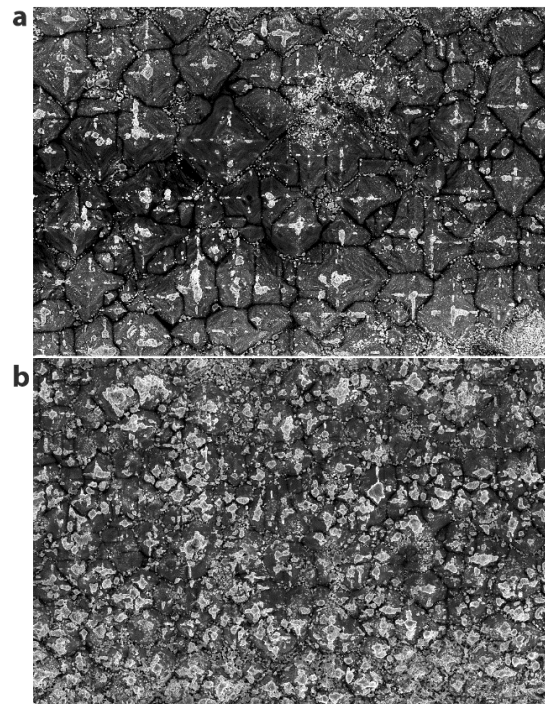


Fig. 5: SEM-picture of samples deposited at a) 680°C and b) 590°C set temperature fired at 795°C.

In order to find a suitable explanation, the contact formation needs to be studied. SEM-images of the area below the Ag bulk are shown in Fig. 5. Both samples deposited at 590°C (bottom) and 680°C (top) are shown.

Each has been fired at 795°C, where the largest difference in ρ_c was observed. When compared to lower deposition temperatures, a large decrease in Ag crystallite density is observed in Fig. 5a. The crystallites are largely centered around pyramid tips and edges. Additionally, large amounts of the previously shown small crystallites can be found on pyramid flanks, while the overall coverage of the Si surface with crystallites remains low. Overall, APCVD AlO_x layers deposited at high temperatures show a similar influence on Ag crystallite growth and thus contact formation as ALD layers. This further implies that the layer density might be responsible for a change in etching behaviour.

The generally low ρ_c for most temperatures shown proves APCVD based AlO_x to be suitable in terms of contact firing. In combination with results regarding the firing stability of the passivation quality of AlO_x deposited in an APCVD reactor, the values shown are promising and enable reproducible use of the presented layers in particular for a PERT cell process.

4 CONCLUSION

AlO_x / $\text{SiN}_y\text{:H}$ stacks containing APCVD based AlO_x can be contacted with contact resistivity values below 1 $\text{m}\Omega\text{cm}^2$ for layer thicknesses between 8-25 nm, which ALD based AlO_x layers only achieve for very low layer thickness. APCVD based layers show Ag crystal formation and thus good contact formation with low contact resistivity independent of layer thickness after firing. This effect is expected to be based on the properties of the AlO_x layer. A deposition temperature study with fixed layer thickness further shows the dependence on layer properties. Excellent contact ($\rho_c < 1 \text{ m}\Omega\text{cm}^2$) through APCVD based AlO_x layers deposited at 590°C can be established at a peak temperature range between (760..805)°C. Contact formation is still possible for profiles with lower thermal load. Contact resistivity is likely predominantly influenced by how Ag crystallites are formed on the silicon surface. How this Ag crystallite growth is influenced by AlO_x layer properties is subject of further investigation.

5 REFERENCES

- [1] J. Engelhardt et al., 35th EUPVSEC, 2018
- [2] R. Hezel et al., J. Electrochem. Soc. 136(2): 518-523, 1989
- [3] S. Fritz et al, physica status solidi (RRL)–Rapid Research Letters, 10(4), 305-309, 2016
- [4] L.E. Black and K.R. McIntosh, Applied Physics Letters 100(20), 202107, 2012
- [5] X.Y. Chen et al., Solar Energy. 158: 917-921, 2017
- [6] S. Fritz et al., IEEE J. Photovoltaics 5(1), 145-151, 2014

6 ACKNOWLEDGEMENTS

Part of this work was supported by the German BMWi under contracts HEAVENLY project (0324226A). The content is the responsibility of the authors.